2025 IEEE 8th International Conference on Soft Robotics (RoboSoft) | 979-8-3315-2020-5/25/$31.00 ©2025 IEEE | DOI: 10.1109/RoboSoft63089.2025.11020817

Variable Stiffness and Variable Size Particles for Reconfigurable Granular Metamaterials

Monica S. Li[1], Brian H. Do[1,2], Caitlin L. Le[1], Corey S. O'Hern[1], and Rebecca Kramer-Bottiglio[1]

***Abstract*— Soft robots can achieve exceptional adaptability through tunable morphological and mechanical properties. Incorporating materials with dynamically adjustable characteristics can enhance this versatility further. Granular metamaterials, consisting of discrete particles with individually variable properties, offer a promising approach to bulk property adaptation by adjusting the properties of constituent particles. This work introduces variable size and variable stiffness (VS^2) particles, in which both particle size and stiffness are independently modulated through concentric pneumatic chambers. We characterize the achievable workspace, mapping particle responses to independent chamber inflation. To demonstrate their use in a granular assembly, we arrange an array of VS^2 particles in a hexagonal packing and validate that behavior in packed configurations aligns with free-space characterizations. This study establishes a foundation for adaptive granular materials and provides a platform for further computational and experimental exploration of 2D and 3D granular metamaterials with tunable properties.**

I. Introduction

Soft robots have the potential to adapt to diverse tasks and environmental changes by adjusting both their morphology and corresponding behavioral control strategies [1]. Extending this adaptability to the material properties of the robot itself can further enhance its functionality. For instance, a robot composed of adaptable materials could reroute forces around a damaged area to achieve self-recovery or modify properties like stiffness and vibration response to suit specific operational needs.

Granular metamaterials—consisting of discrete particles—are an intriguing platform for creating adaptable materials, as individual particle properties can be widely tuned to achieve different material responses [2]. While stimuli-responsive materials traditionally adjust only one property, such as stiffness, in response to a specific input, mechanical metamaterials offer the potential for broader or novel responses [3]. However, most metamaterials have been designed as continuum solids or fixed structures, limiting them to static, rather than adaptive, behaviors. Developing assemblies of active particles that can continuously and dynamically adjust in stiffness, size, and shape would unlock structural reconfigurations and a greater range of bulk property adaptations.

[1]Department of Mechanical Engineering & Materials Science, Yale University, New Haven, CT 06520, USA. (email: rebecca.kramer@yale.edu)

[2]Collaborative Robotics and Intelligent Systems (CoRIS) Institute, Oregon State University, Corvallis, OR 97311, USA

This material is based upon work supported by the National Science Foundation under the DMREF program (award number: 2118810). C.L. was supported by a NASA NSTGRO Fellowship (80NSSC24K1339).

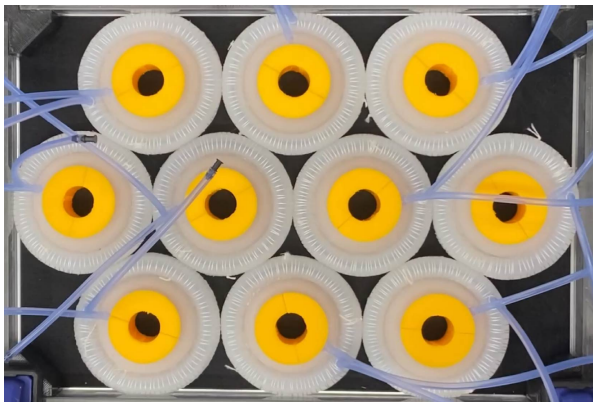

Fig. 1. Packed configuration of variable stiffness and variable size (VS^2) particles, which are soft pneumatic particles with independently controllable stiffness and size.

We define a bulk property as a metric where the material is evaluated as a whole, such as compressive and shear stiffness. Recent work has also demonstrated that granular metamaterials can be designed to exhibit computational behavior, implementing input-output relations such as logic gates, further broadening their functional capabilities [4].

Prior work on adaptive particle assemblies, such as robotic matter and particle jamming, has primarily focused on reconfiguring inert particles within an assembly [5]–[7]. Examples where bulk property adaptation is driven by individual particle adjustments are relatively rare. In cases where particles exhibit changes, the focus has often been on a single attribute, such as size. For example, Eristoff *et al*. developed granular actuators with particles that expand volumetrically [8], while Li and Batra *et al*. demonstrated robotic particles capable of individually changing diameter for collective translation [9]. Witthaus *et al*. explored particles that change stiffness to modify force chains across the assembly [10].

We posit that a material composed of particles capable of adapting both their stiffness and size could achieve more versatile and efficient bulk property adaptations. Furthermore, in dynamic systems, the choice of adaptation pathways is crucial. Just as there exist infinite possible paths for a locomotion robot, there analogously exists infinite possible grain-level adaptations to achieve a desired time-ordered property state progression for a granular material. What is the most efficient adaptation path? Is it energetically favorable to wildly adapt one grain or to mildly adapt many grains, if both options will produce the same overall property state?

In this work, we present a particle design that enables

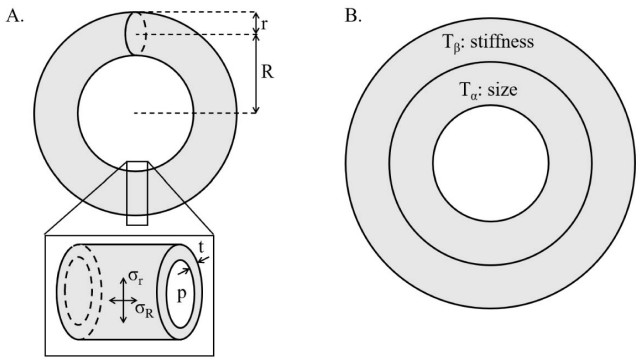

Fig. 2. Schematic diagrams. (A) Single torus geometry, defined by two dimensions, the major radius R and minor radius r. A cross-section of the torus depicts wall thickness t and inflation pressure p. (B) Concept schematic of the VS^2 particle. The inner torus T_α dictates particle size, and the outer torus T_β controls stiffness.

us to address these questions (Fig. 1). Moving beyond previous active particle designs limited to either stiffness or size modulation, our design enables independent control over both. We denote the particles as variable stiffness and variable size particles, or VS^2 particles. These soft robotic particles use pneumatic pressure as a mechanical input to modulate stiffness and size independently. Typically, increasing pressure in soft inflatable structures results in an expansion if unconstrained, or increased stiffness if constrained. Recent results have shown that geometry can further tune this stiffness-pressure relationship [11]. Building on these insights, we developed particles with a concentric chamber structure analogous to stacked pouches [12], [13], featuring two rings with distinct external constraints, allowing stiffness and size to be adjusted independently. This advancement paves the way for more dynamic and adaptive behaviors in granular metamaterials.

In the near term, the VS^2 particles will serve as benchmarks for validating computational metamaterial simulations. To address the challenges of modeling 3D particle interactions, we first developed "2D" particles, with stiffness and size changes constrained to a two-dimensional plane. Future work will focus on refining the simulations for 3D interactions and developing fully 3D particles with adaptable stiffness and size.

II. Theory & Design

When inflating a structure, the pressure acts in all directions normal to the inner surface. Soft, inflatable structures intended for 2D behavior should reduce the effect of out-of-plane deformations due to pressure. We designed the VS^2 particle with two concentric toroidal-shaped pressure chambers. The geometry of a ring torus, or *donut*, with a hollow interior, reduces the change in the out-of-plane dimension due to inflation relative to other circular structures without a center hole. Further, the absence of edges or corners on a torus reduces stress concentrations and non-idealized deformations during inflation. Geometrically, a torus exhibits 2D inflation behavior while existing in 3D space.

TABLE I

Dimensions of this VS^2 particle (mm). SL: Strain-limiting

	Major radius R	Minor radius r	Thickness t	SL?
T_α	13	5	3	No
T_β	26	3	2	Yes

A ring torus is defined by its major radius R and minor radius r, where $R > r$ (Fig. 2A). The cross-sectional view shows that the torus is hollow and pressurized to gauge pressure p, with uniform wall thickness t (Fig. 2A, inset). In our design, the torus walls are elastic, and increasing internal pressure increases the torus size. The following derivation assumes small deformations and uniformly elastic walls, and is intended to provide insight into the mechanical behavior of the VS^2 particle. We calculate wall hoop stress along the minor circumference σ_r and axial stress along the major circumference σ_R (Fig. 2A, inset):

$$\sigma_R = \frac{pr}{2t},\ \sigma_r = 2\sigma_R. \tag{1}$$

Stress σ and strain ε are related by Young's modulus, E: $\sigma = E\varepsilon$. We define strain as the change in radius divided by the original radius, where the original radius is the uninflated radius of the particle: $\varepsilon_R = \Delta R/R_0$. We can thus rewrite the major radius as the uninflated radius R_0 plus another term that is proportional to strain along the major radius ε_R:

$$R = R_0 + \Delta R = R_0 + R_0\varepsilon_R. \tag{2}$$

We omit the analogous equations for the minor radius for brevity.

Both the minor and major radii increase when pressure increases. Rearranging the above equations, the total radius of the particle as a function of pressure is

$$R + r = (R_0 + r_0) + \frac{r_0}{2Et}(R_0 + 2r_0)p. \tag{3}$$

Inflating the torus increases the total radius. This size increase is more sensitive to the minor radii dimension by a factor of two, which comes from Eqn. 1.

The VS^2 particle design requires independently controlled stiffness and size. As such, we have two connected, concentric tori that are independently inflatable. We refer to the inner torus that dictates size as T_α and the outer torus that modulates particle stiffness as T_β (Fig. 2B). The walls of T_β have a strain-limiting layer that restricts the volumetric expansion of the torus. Thus, inflating T_β increases stiffness [14]. The total VS^2 particle radius is

$$R_{tot} = R_\alpha + r_\alpha + 2r_\beta. \tag{4}$$

The particle must increase in size with inflation of T_α, so the wall of T_β cannot be entirely inelastic. Both Eqn. 3 and Eqn. 4 provide a framework to design particles of the described concept geometry.

III. Fabrication methods

We modified the theoretical particle design for physical implementation. Fig. 3 shows the VS^2 particle in computer-aided design (CAD) and physically realized. Two tori and the rigid center comprise one VS^2 particle.

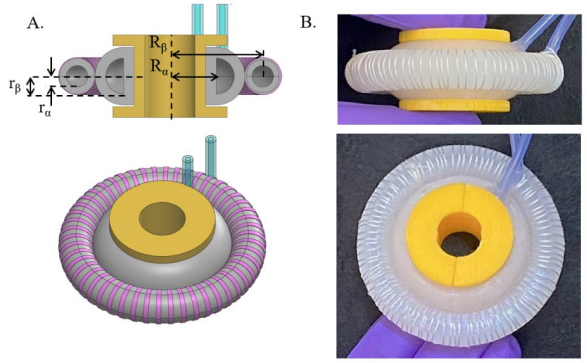

Fig. 3. Assembled VS^2 particle with two toroidal pressure chambers and a rigid inner support. (A) Section and isometric view from CAD. (B) Side and isometric view images of realized particle.

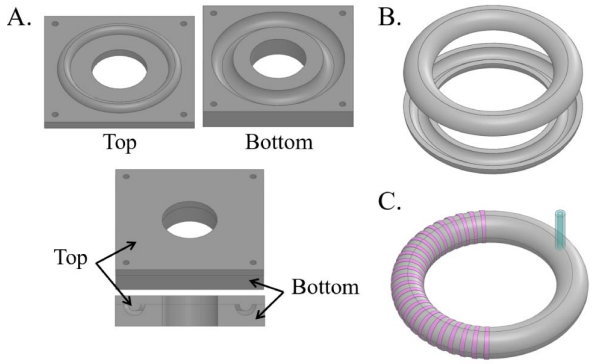

Fig. 4. Fabrication steps for T_β. (A) Additively manufactured negative molds for casting silicone. (B) Two torus halves to be glued together. (C) Inserted silicone inlet tube and wrapped strain-limiting string (pink).

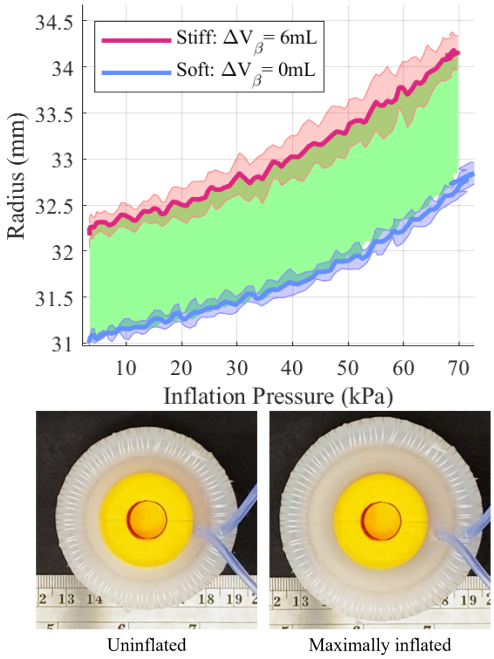

Fig. 5. Size characterization, plotted as particle radius versus inflation pressure of T_α (N=5). T_α is cyclically inflated with 20 mL to 66 kPa and deflated, while T_β is uninflated (soft, blue line) or inflated with 6 mL to 48 kPa (stiff, pink line). The region between the two curves represents the set of achievable radii by varying T_β inflation (shaded green). Photos show an example VS^2 particle with both T_α and T_β uninflated on the left and both maximally inflated on the right.

Inward expansion of T_α upon inflation does not change particle size, and the minor cross-section of T_α is modified to a D-shape and constrained by a rigid center. The rigid center restricts inward and out-of-plane expansion, analogous to a bicycle rim. The rigid center has a hollow core, which can be utilized for housing electronic components in future untethered designs.

To decouple stiffness and size changes in the VS^2 particles, we added a strain-limiting layer to constrain expansion of r_β, while R_β is free to expand with inflating T_α. The wall thickness and minor radius of T_α is greater than that of T_β, so the main driver for particle size is the inflation of T_α and not T_β. We list the dimensions pictured in Fig. 3A of the VS^2 particle in Table I.

We fabricated the VS^2 particles using casting and rapid prototyping techniques, shown for T_β in Fig. 4. First, we designed and 3D printed (PRUSA i3 MK3) negative molds (Fig. 4A). The two-part mold makes one-half of the hollowed torus shape, and dowel pins align the two parts. We poured silicone elastomer (Smooth-On DragonSkin 10 Slow, Shore 10A) into the bottom mold. The uncured silicone is vacuum-degassed before the top mold is pressed into the elastomer. After curing, we removed the formed silicone half-torus and glued them together along the flat face using a silicone adhesive (Smooth-On Sil-Poxy) (Fig. 4B). We inserted and glued a silicone tube (1/8" outer diameter, Shore 50A) to the top of the torus and added the strain-limiting layer by winding an effectively inelastic string (nylon thread, 210D/3), approximately 90 revolutions per particle (Fig. 4C). The torus is fully sealed except for the open end of the silicone tubing. T_α is similarly fabricated. We used silicone adhesive and a rigid alignment fixture to bind T_α and T_β along the center line. The rigid center was 3D printed and inserted into the particle's center.

IV. Characterization

A. Variable Size

We characterized particle size based on inflation pressure for five individual VS^2 particles. Each VS^2 particle's size torus, T_α, was inflated with an additional 20 mL of air, generating approximately 66 kPa of pressure, at which point both the inflation pressure and size were measured. T_β was either uninflated or maximally inflated with 6 mL of air, or approximately 48 kPa. The inflation of T_β was limited due to out-of-plane, monkey-saddle-shaped deformations observed at higher pressures. Particle size was measured using video data (1080p, RGB) analyzed via MATLAB's *imfindcircles()* function, assuming a circular VS^2 particle shape. Pressure data was recorded for one inflation cycle (approximately 30 sec duration) at a 2 Hz sampling rate with an analog pressure gauge (3.4-103 kPa range, Carbo Instruments).

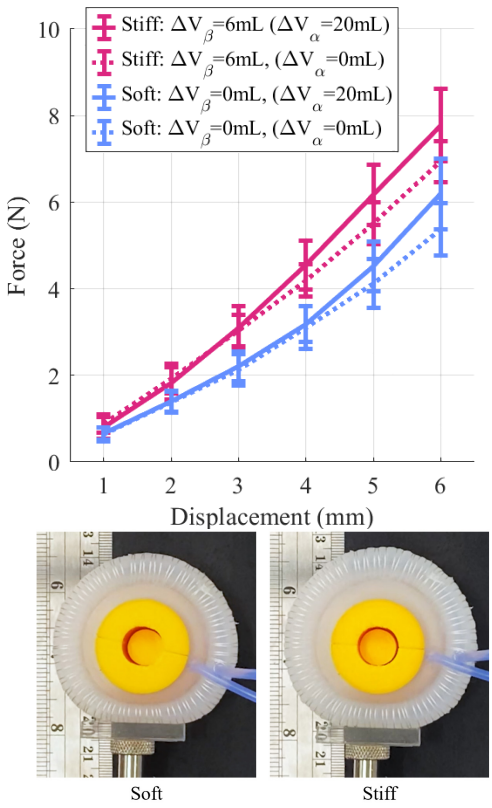

Fig. 6. Stiffness characterization. Force versus displacement for uninflated and maximally inflated tori (N=5). Inflation of T_α increases particle size, and inflating T_β increases stiffness but also size. Photos show a soft (uninflated T_β) and stiff (maximally inflated T_β) VS^2 particle undergoing 6 mm linear compression for uninflated T_α.

Fig. 5 shows the average VS^2 particle size for one inflation cycle of T_α at both the minimum and maximum inflation pressures of T_β. The inset shows T_α in its uninflated and maximally inflated states, while T_β is fully inflated.

Increasing the pressure in either chamber increases the particle size from its uninflated radius of 31 mm. Inflating T_α alone results in a radius change of 1.8 mm (5.8%) when T_β is uninflated and 2.0 mm (6.2%) when T_β is maximally inflated. Inflating T_β increases the total radius up to 1.2 mm (3.9%) when T_α is uninflated. The maximum radius increase is 3.2 mm (10%). Within this, the particle can access its entire stiffness range for radii between 32.2 and 32.8 mm, or 0.6 mm (1.9%) range.

B. Variable Stiffness

We characterized the stiffness-tuning abilities of five VS^2 particles using linear compression. Each particle was mounted at the center, and compression was applied incrementally on the side up to 6 mm, at 1 mm increments, with two measurements taken per particle. A flat acrylic piece was mounted to a force gauge (Torbal FC500, 500 N $\times$ 0.1 N) to ensure uniform displacement across the particle surface. Stiffness was measured in four inflation configurations: with combinations of T_α and T_β each in their uninflated and maximally inflated states.

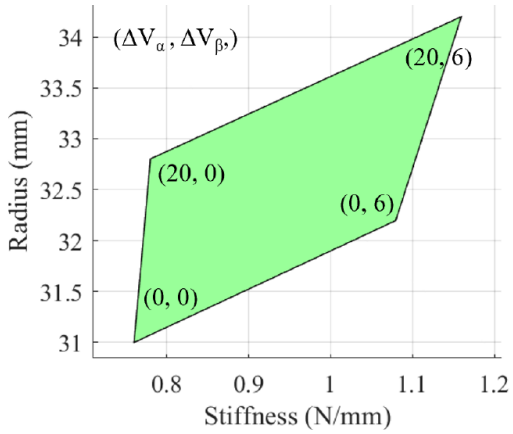

Fig. 7. The approximate total achievable workspace of area and stiffness for a VS^2 particle. The volumetric inflation ΔV at each vertex is listed for T_α and T_β.

TABLE II

VS^2-PARTICLE STIFFNESS k FOR THE MAXIMAL AND MINIMAL INFLATION RANGE (N=5).

ΔV_α (mL)	ΔV_β (mL)	k [N/mm]
0	0	0.76 $\pm$0.14
20	0	0.78 $\pm$0.16
0	6	1.08 $\pm$0.14
20	6	1.16 $\pm$0.20

Fig. 6 shows the force measurements for varying displacements. Stiffness k is calculated from the slope of a least-squares fit of the force-displacement curve in the linear region, which we define as a displacement range of 1–3 mm (Table II). Under small deformations in this linear region, stiffness depends solely on the inflation of T_β and is independent of the inflation of T_α. The particles have an average stiffness of 0.77 N/mm when uninflated and 1.12 N/mm when inflated, resulting in a stiffness variation of 45%. For displacements greater than 3 mm, the inflation of T_α begins to have an effect, as inflating T_α increases both stiffness and size.

We suspect that linear displacements less than 3 mm primarily deform T_β, while larger displacements also deform T_α, as reflected in the results shown in Fig. 6. Additionally, we propose that inflating T_α deforms the cross-sectional shape of T_β.

We combined the results from the stiffness and size characterizations to create a workspace for the VS^2 particle (Fig. 7). The four corners correspond to the uninflated and maximally inflated pressures for both T_α and T_β. Any radius and stiffness within these bounds can be achieved by varying the pressures applied to both tori. Future work will focus on discretizing this workspace and mapping the numerical inflation values to corresponding stiffness and size.

V. Demonstration in Granular Assembly

The VS^2 particles are intended for use in a granular packing, where neighboring particles and wall boundaries constrain expansion and cause deformation. To qualitatively

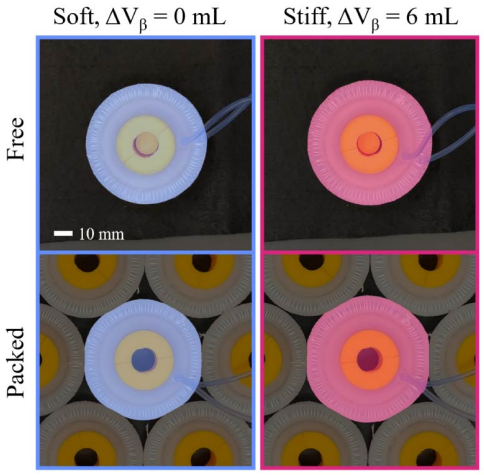

Fig. 8. Top-down view of masked VS^2 particle in free and packed configurations, for maximally inflated T_α and varying T_β inflation for stiffness. Scale bar is 10 mm.

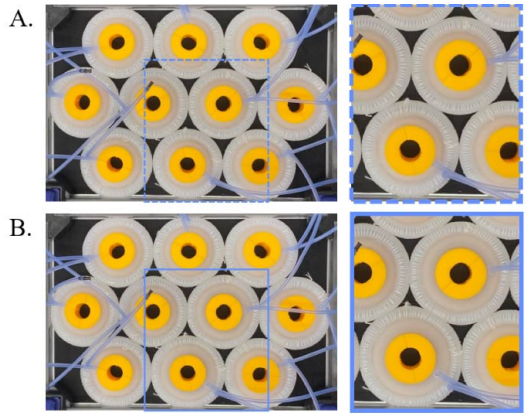

Fig. 9. Variable size in the granular assembly. (A) All particles are uninflated. (B) Two particles, located in the bottom row center and middle row center-right, are maximally inflated. The closeup view focuses on the two size-changing particles.

validate this intended use case, we assembled particles in a packed configuration. A rigid containment box was made from laser-cut acrylic and additively manufactured corner pieces, and dimensioned to keep the particles in contact when uninflated. We placed ten VS^2 particles in the box in a hexagonal packing arrangement, where each particle is in contact with at most six other surfaces. We then inflated a single particle to observe how its behavior in the packed configuration differed from the free, unconstrained state.

We evaluated the size and shape deformation of a single inflated particle, both unconstrained and packed with six neighboring particles. Shape deformation was assessed using the root-mean-squared error (RMSE) of the particle radius compared to a circle. We define the radius RMSE as:

$$\text{RMSE} = \sqrt{\frac{\sum_i (r_i - \bar{r})^2}{N}} \tag{5}$$

where r_i is the distance between point i on the perimeter and the centroid, $\bar{r}$ is the average distance between the perimeter and centroid, and N is the number of points. The RMSE of a perfect circle is zero. The more non-circular a shape, the higher its RMSE.

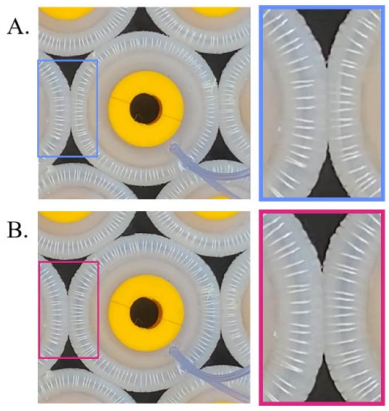

Fig. 10. Variable stiffness in the granular assembly while inflation volume and nominal size are kept constant. The particle is (A) soft then (B) stiff. The closeup shows an enlarged view of particle-particle contact and the change in the right particle's r_β.

We evaluated the particle at maximally inflated T_α, for both minimally and maximally inflated T_β, and report the mean values from three trials for both the free and packed configuration in Table III. The particle size as average radius and the shape deformation as RMSE are both calculated from the mask overlaid in Fig. 8. In the packed configuration, the particle's average radius was reduced 1.2% from its unconstrained radius for the soft state and 1.5% for the stiff state. Comparing the normalized shape deformation, the particle's RMSE/$\bar{R}_{tot}$ value more than doubles in the packed configuration, increasing by a factor of 2.3 for the soft state and 2.4 for the stiff state. The particles are visibly deformed and non-circular in the packed configuration. The similarity between soft and stiff in the above reported values is likely due to the size-stiffness coupling of T_β inflation; if the particle size is constant and the stiffness increases, we would expect a smaller change in RMSE/$\bar{R}_{tot}$.

TABLE III
MEAN TOTAL RADIUS $\bar{R}_{tot}$, RMSE, AND NON-DIMENSIONALIZED RMSE COMPARING PACKING CONFIGURATION AND T_β INFLATION AVERAGED OVER FIVE MEASUREMENTS.

Config.	ΔV_β (mL)	$\bar{R}_{tot}$ (mm)	RMSE (mm)	RMSE/$\bar{R}_{tot}$
Free	0	32.1	0.116	0.361%
Free	6	33.6	0.142	0.424%
Packed	0	31.7	0.383	1.21%
Packed	6	33.1	0.475	1.44%

Next, we qualitatively assessed more complex adaptations in a granular packing. All the particles started uninflated (Fig. 9A), and then we maximally inflated T_α for the center particle on the bottom row and then the center-right particle in the middle row (Fig. 9B). When T_α is inflated, the particle increases in size, expanding into the open space and deforming at the contact of neighboring particles and walls. We demonstrated the size variation of the VS^2 particles in a packed configuration behaves as intended. Inflating T_β

increases both stiffness and area, making it challenging to observe changes in stiffness independently from size.

To isolate the effects of particle stiffening within a packed configuration, we varied the stiffness of a central particle in the assembly while maintaining an approximately constant particle size by holding the total inflation volume fixed. The total inflation volume was held constant, $\Delta V_\alpha + \Delta V_\beta = 20$ mL, while ΔV_β was varied between 0 mL (Fig. 10A) and 6 mL (Fig. 10B) to control the stiffness. Qualitatively, the stiff particle maintains a more circular shape and displaces neighboring particles more than the softer, more deformable particle. This demonstration highlights the potential of the VS^2 particle design, suggesting that further characterization could enable us to further decouple variable stiffness from size changes and, more broadly, to map inflation to precise stiffness and size combinations.

Taken together, these preliminary results suggest that the VS^2 particle could be used as a platform to study adaptive granular materials.

VI. Conclusion

We designed and fabricated the VS^2 particle, a soft pneumatic particle that has independently inflated toroidal chambers that control stiffness and size. The particle size is coupled to the inflation of both tori, with the inner torus offering a greater size range. The particle stiffness depends on the inflation pressure of the outer torus. In a packed configuration, these particles can exhibit variable stiffness and variable size behaviors, providing a platform to probe questions around adaptive granular metamaterials.

To enhance the functionality of the VS^2 particles, we will focus on improving the fabrication processes to achieve more consistent behavior across future iterations. Currently, the silicone adhesive is much stiffer than the torus walls, so varying the amount applied can influence the overall performance. By optimizing the uniformity of the strain-limiting layer, we can further enhance consistency. Additionally, increasing the density of string wrapping on T_β or reducing r_β could mitigate size changes while preserving the variable stiffness behavior. Conversely, with a lower string winding density and higher inflation pressures, the silicone chamber may expand beyond the string constraints, leading to bulging or rippling effects. We also plan to integrate a pneumatic control system to facilitate simultaneous inflation and deflation of the particles, streamlining operations and enhancing responsiveness. The current particle-box configuration is limited by the total assembly pressure or the packing fraction. Excessive assembly pressure can elevate contact stresses, leading to particles dislodging from the box. To address this, we can either maintain the total pressure or stress within the box or implement constraints to limit out-of-plane motion, or a combination of both.

Studying the individual behaviors of active particles that can vary in stiffness, size, and shape, as well as the overall dynamics of their assembly as a bulk material, will have substantial implications. Insights gained from this research could advance our understanding of adaptive granular materials, influencing fields such as soft robotics, adaptive structures, and bio-inspired design. By exploring the interplay between individual particle characteristics—such as stiffness and size—and their collective behavior, we can uncover efficient adaptations for adaptive granular metamaterials.

References

[1] D. Shah, B. Yang, S. Kriegman, M. Levin, J. Bongard, and R. Kramer-Bottiglio, "Shape changing robots: bioinspiration, simulation, and physical realization," *Advanced Materials*, vol. 33, no. 19, p. 2002882, 2021.

[2] B. Jenett, C. Cameron, F. Tourlomousis, A. P. Rubio, M. Ochalek, and N. Gershenfeld, "Discretely assembled mechanical metamaterials," *Science Advances*, vol. 6, no. 47, p. eabc9943, 2020.

[3] K. Bertoldi, V. Vitelli, J. Christensen, and M. Van Hecke, "Flexible mechanical metamaterials," *Nature Reviews Materials*, vol. 2, no. 11, pp. 1–11, 2017.

[4] P. Welch, M. Li, S. Beaulieu, A. Xia, D. Wang, M. Goyal, A. Parsa, C. O'Hern, R. Kramer-Bottiglio, and J. Bongard, "Greater AI Design Control Aids Evolution of Computational Materials," in *International Conference on the Applications of Evolutionary Computation (Part of EvoStar)*. Springer, April 2025.

[5] B. Saintyves, M. Spenko, and H. M. Jaeger, "A self-organizing robotic aggregate using solid and liquid-like collective states," *Science Robotics*, vol. 9, no. 86, p. eadh4130, 2024.

[6] J. Wang, G. Wang, H. Chen, Y. Liu, P. Wang, D. Yuan, X. Ma, X. Xu, Z. Cheng, B. Ji *et al.*, "Robo-matter towards reconfigurable multifunctional smart materials," *Nature Communications*, vol. 15, no. 1, p. 8853, 2024.

[7] H. M. Jaeger, "Celebrating soft matter's 10th anniversary: Toward jamming by design," *Soft Matter*, vol. 11, no. 1, pp. 12–27, 2015.

[8] S. Eristoff, S. Y. Kim, L. Sanchez-Botero, T. Buckner, O. D. Yirmibeşoğlu, and R. Kramer-Bottiglio, "Soft actuators made of discrete grains," *Advanced Materials*, vol. 34, no. 16, p. 2109617, 2022.

[9] S. Li, R. Batra, D. Brown, H.-D. Chang, N. Ranganathan, C. Hoberman, D. Rus, and H. Lipson, "Particle robotics based on statistical mechanics of loosely coupled components," *Nature*, vol. 567, no. 7748, pp. 361–365, 2019.

[10] S. Witthaus, A. Parsa, N. Pashine, J. Zhang, A. Mackeith, M. D. Shattuckc, J. Bongard, C. S. O'Hern, and R. Kramer-Bottiglio, "Evolution of Adaptive Force Chains in Reconfigurable Granular Metamaterials," *Unpublished Manuscript*, 2024.

[11] N. Pashine, R. Baines, D. Wang, M. Goyal, C. O'Hern, and R. Kramer-Bottiglio, "Varying the stiffness of inflating balloons via geometry," *Bulletin of the American Physical Society*, 2024.

[12] B. H. Do, A. M. Okamura, K. Yamane, and L. H. Blumenschein, "Macro-Mini Actuation of Pneumatic Pouches for Soft Wearable Haptic Displays," in *2021 IEEE International Conference on Robotics and Automation (ICRA)*, 2021, pp. 14 499–14 505.

[13] C. M. Nunez, B. H. Do, A. K. Low, L. H. Blumenschein, K. Yamane, and A. M. Okamura, "A Large-Area Wearable Soft Haptic Device Using Stacked Pneumatic Pouch Actuation," in *2022 IEEE/RSJ International Conference on Intelligent Robots and Systems (IROS)*, 2022, pp. 591–598.

[14] B. Wiegand, "NOTES on TIRE BEHAVIOR, Rev. D," May 2015.